Supplementary Information (SI) for Inorganic Chemistry Frontiers.

Supplementary Information

Multi-structured and Ligand Modified NiFe LDH with Self-Optimization for Efficient Oxygen Evolution Reaction.

Zi-Ye Liu, Jiu-Jiu Ge and Ji-Ming Hu*

Department of Chemistry, Zhejiang University, Hangzhou 310058, P. R. China

*: Corresponding author. E-mail: kejmhu@zju.edu.cn.

1. Characterization

The self-optimized LDH-MOF74@NF electrode was rinsed with deionized water before characterization to remove KOH and NaCl. Except for transmission electron microscopy (TEM), all characterization techniques were used directly on the nickel foam electrodes. The nickel foam was cut into small pieces and subjected to ultrasonic treatment in few EtOH for 1 hour. The supernatant was then collected and dropped onto a grid for observing the sample morphology, elemental distribution, and structure in TEM and HRTEM.

The morphology of electrodes was characterized using field emission scanning electron microscopy (SEM, SU8010, Hitachi). Transmission electron microscopy (TEM, HT7700, Hitachi) and high-resolution transmission electron microscopy (HRTEM, 2100F, Jeol) coupled with energy-dispersive X-ray spectroscopy (EDS, OXFORD 80T, Oxford Instruments Plc.) were used to investigate the nanostructure and element distribution of MOF-74, LDH-MOF74 before and after OER. X-ray diffraction patterns were obtained by X-ray diffractometer (XRD, SmartLab, Rigaku Electric Co.) with Cu Kα radiation. Th infrared spectra were obtained using an ATR-IR spectrometer (IR, Nicolet iS10, ThermoFisher Scientific). The spectra were recorded in the range of 4000 ~ 400 cm^{-1}. The Raman spectra was obtained by Laser confocal Raman spectroscopy (LabRAM HR evolution, HORIBA Jobin Yvon). The measurements were carried out with an excitation wavelength of 532 nm. Raman spectra were used for in-situ electrochemical tests as well. The microscale infrared spectra were acquired by microscale infrared spectrometer (iN10 MX, ThermoFisher Scientific). X-ray photoelectron spectroscopy (XPS, Thermo ESCALAB 250Xi, ThermoFisher Scientific) was used to analyze the elemental composition of the prepared electrodes. Inductively Coupled Plasma Mass Spectrometry (ICP-MS, NexION 2000, PerkinElmer Health Science Inc.) was performed to determine the elemental composition of the samples The electrochemical test was evaluated by CHI 760e electrochemical workstation (CH Instruments Inc.). Electrochemical impedance spectroscopy (EIS) data were collected using a VersaStat 3F (AMETEK).

2. Density functional theory (DFT) calculations

The Vienna Ab-initio Simulation Package (VASP) was employed to conduct all Density Functional Theory (DFT) calculations. The Perdew-Burke-Ernzerhof (PBE) exchange-correlation functional, employing the generalized gradient approximation (GGA) method with Grimme D3 dispersion correction, was utilized in this study. The projected augmented wave (PAW) method was utilized to describe core-valence interactions in all DFT calculations. The energy cutoff for plane wave expansions was set to 450 eV, and the 1×1×1 Monkhorst-Pack grid k-points were used to sample the Brillouin zone integration for structural optimization of surface structures. Structural optimization was carried out with energy and force convergence criteria setting at 1.0×10-5 eV and 0.02 eV Å-1, respectively.

3. Supplementary data

Table S1. Overpotential of NiFe LDH based OER electrode in 1 M KOH and alkaline seawater

Electrode	Electrolyte	Overpotential (100 mA cm^{-2})	Electrolyte	Overpotential (100 mA cm^{-2})	Reference
LDH-MOF74@NF	1 M KOH	**244 mV**	1 M KOH 0.62 M NaCl	**256 mV**	**This work**
NiFe-LDH-6-4/CC	1 M KOH	252 mV	1 M KOH 0.5 M NaCl	301 mV	[1]
NiFe LDH-CAN3	1 M KOH	257 mV	1 M KOH 0.5 M NaCl	270 mV	[2]
Co1.98-NiFe LDH@NF	1 M KOH	290 mV	1 M KOH 0.5 M NaCl	309 mV	[3]
NiFeCo-NF	1 M KOH	249 mV (10 mA cm^{-2})	1 M KOH 0.5 M NaCl	304 mV	[4]
la-S-NiFe-LDH/NFF	1 M KOH	245 mV	1 M KOH 0.5 M NaCl	253 mV	[5]
N-CDs/NiFe-LDH/NF	1 M KOH	260 mV	1 M KOH 0.5 M NaCl	285 mV	[6]
NiFe-LDH/MOF/NF	1 M KOH	275 mV	1 M KOH 0.5 M NaCl	307 mV	[7]
NiCo-LDH/NiFe-LDH-30@NF	1 M KOH	240 mV	1 M KOH 0.5 M NaCl	333 mV	[8]
Li-doped NiFe-LDH/*g*-C_3N_4	1 M KOH	276 mV	1 M KOH 0.5 M NaCl	319 mV	[9]
Cr-OH/NiFeLDH@NF	1 M KOH	248 mV	1 M KOH 0.5 M NaCl	279 mV	[10]

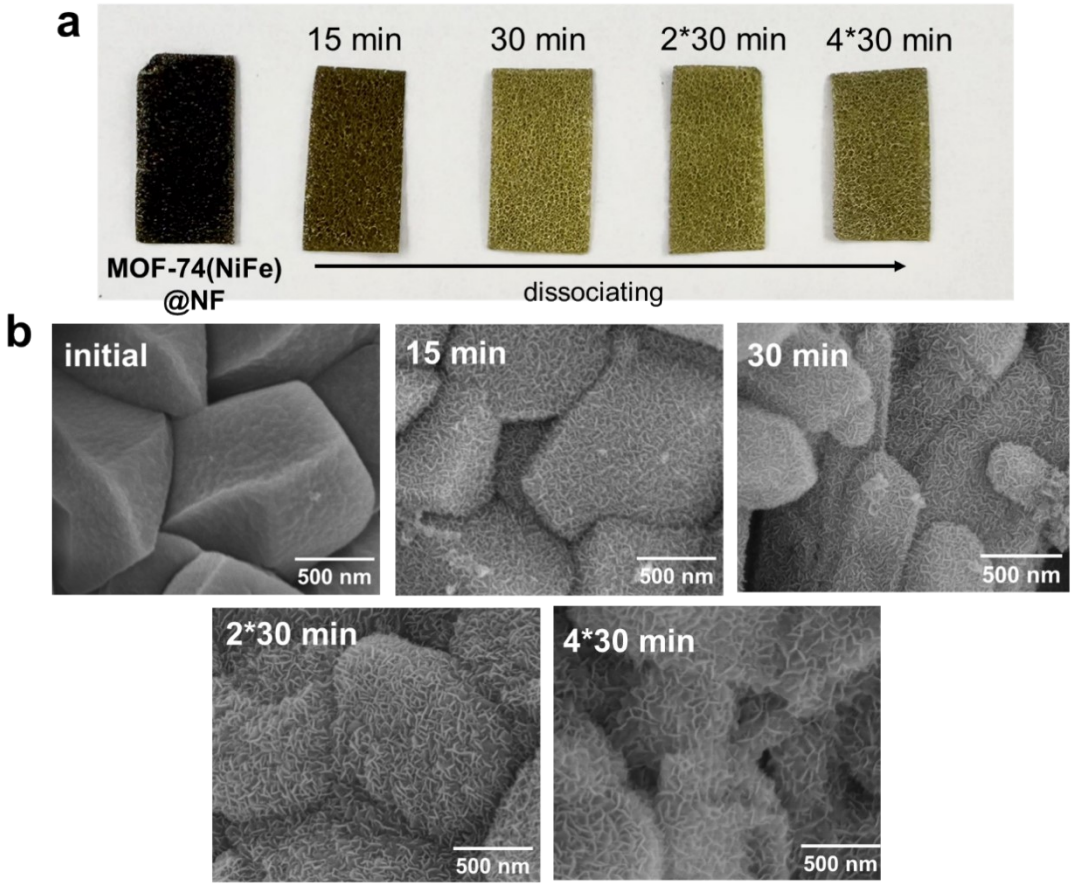

Figure S1. (a) optical images and (b) SEM images of LDH-MOF74@NF with different dissociation times.

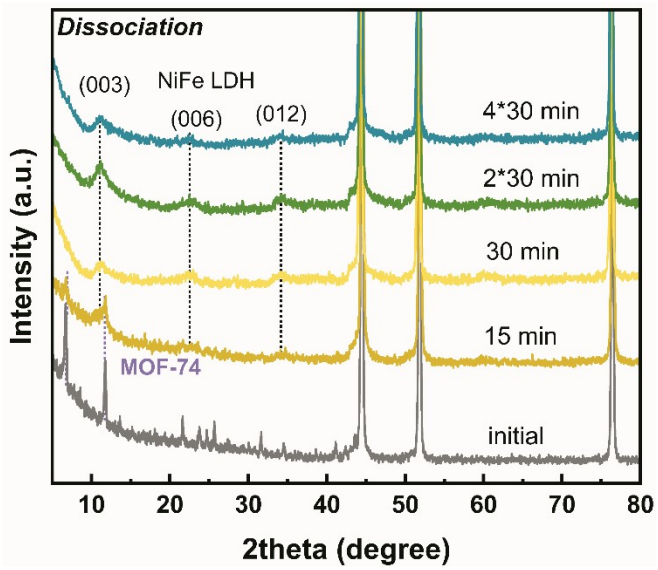

Figure S2. XRD patterns of LDH-MOF74@NF with different dissociation times.

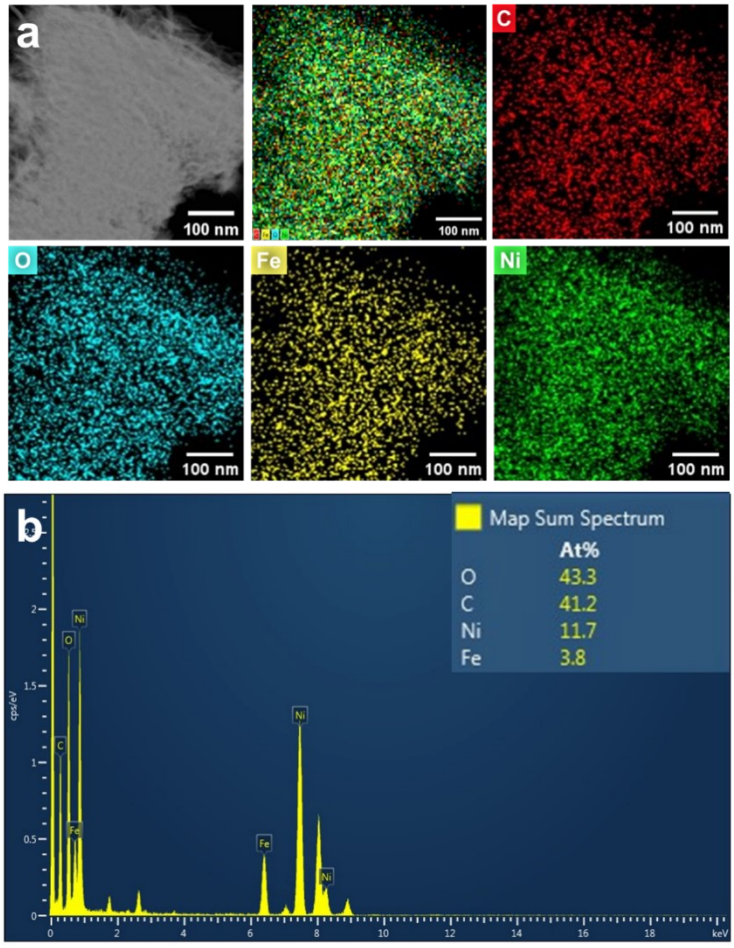

Figure S3. HRTEM-EDS mapping results of LDH-MOF74

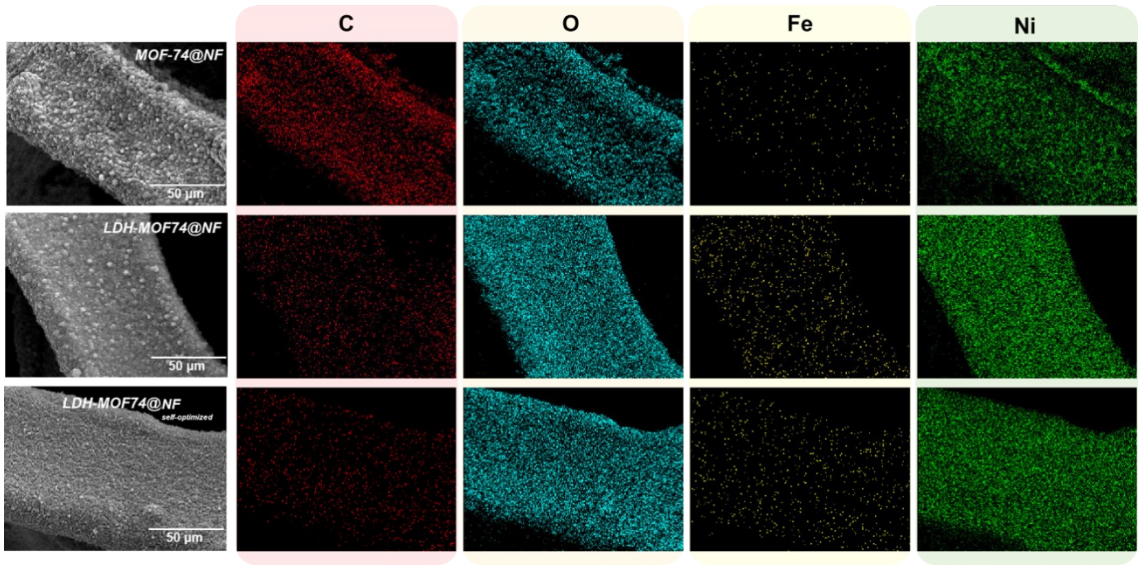

Figure S4. SEM-EDS mapping results of MOF-74@NF and LDH-MOF74@NF before and after self-optimization.

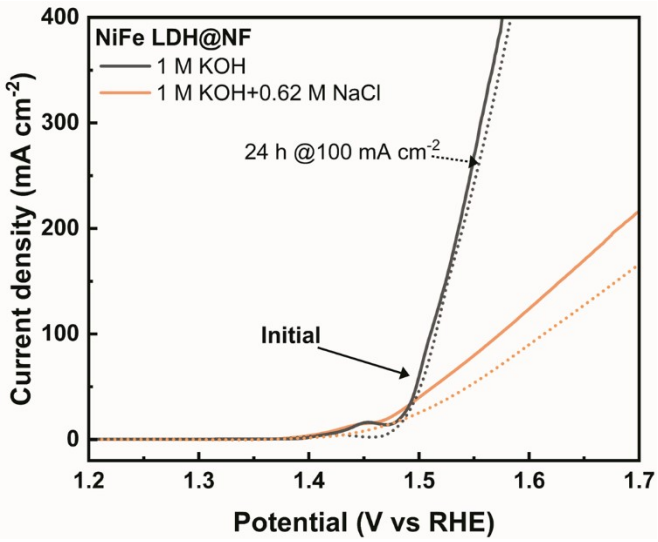

Figure S5. LSV curves of NiFe LDH@NF with performing at 100 mA cm^{-2} in 1 M KOH solution for 24 hour.

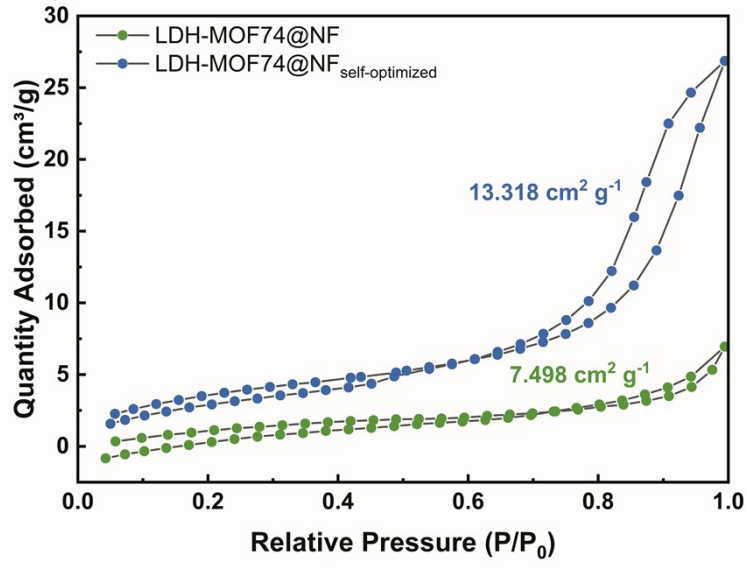

Figure S6. BET measurement of LDH-MOF74@NF before and after self-optimization.

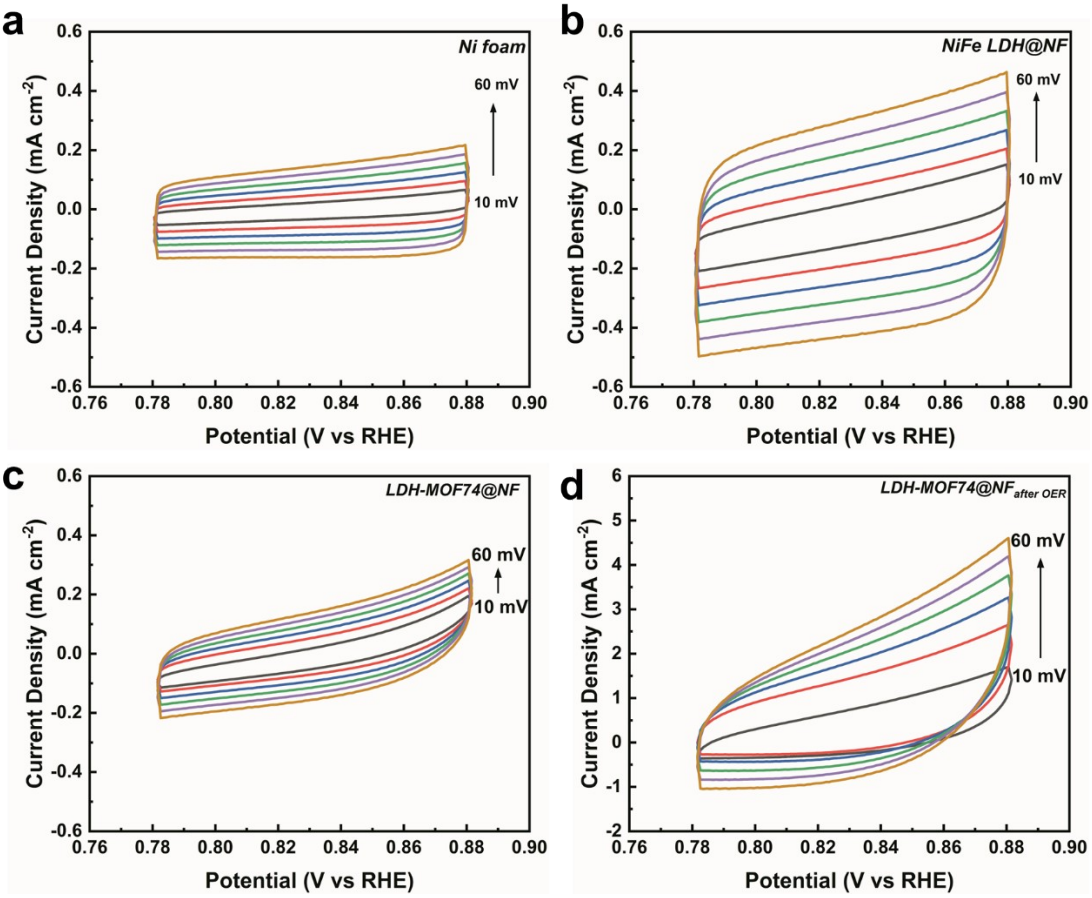

Figure S7. Cyclic voltammetry (CV) curves of (a) nickel foam, (b) NiFe LDH@NF, (c) LDH-MOF74@NF and (d) optimized LDH-MOF74@NF at different scan rates under non-Faradaic conditions.

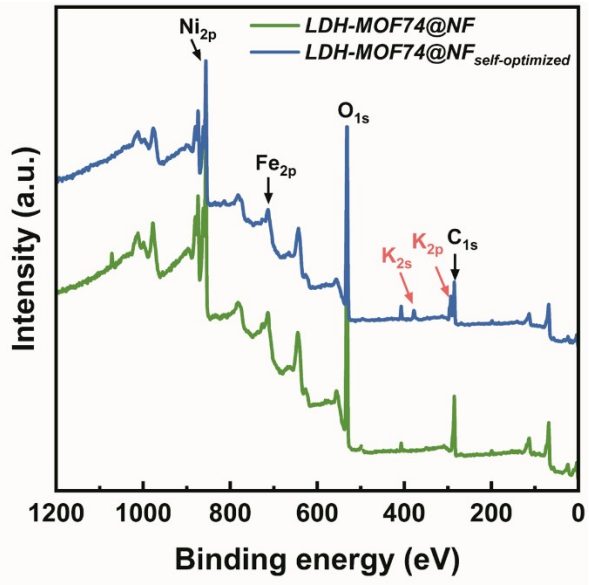

Figure S8. XPS spectra of LDH-MOF74@NF before and after OER.

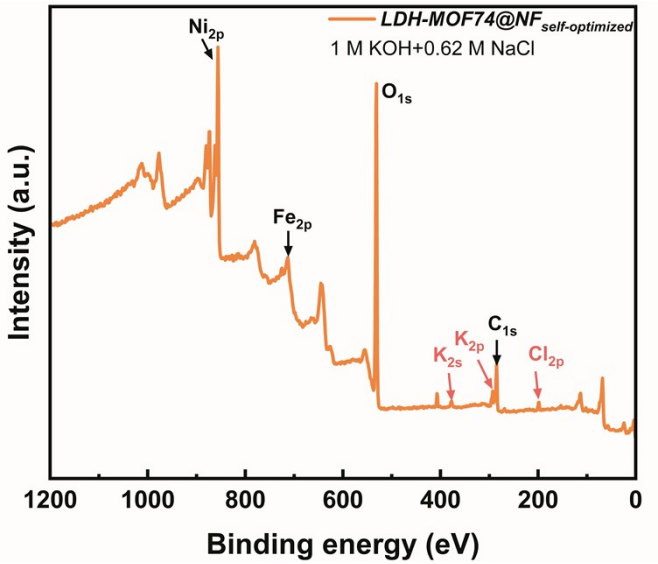

Figure S9. XPS spectra of LDH-MOF74@NF after OER test in 1 M KOH + 0.62 M NaCl.

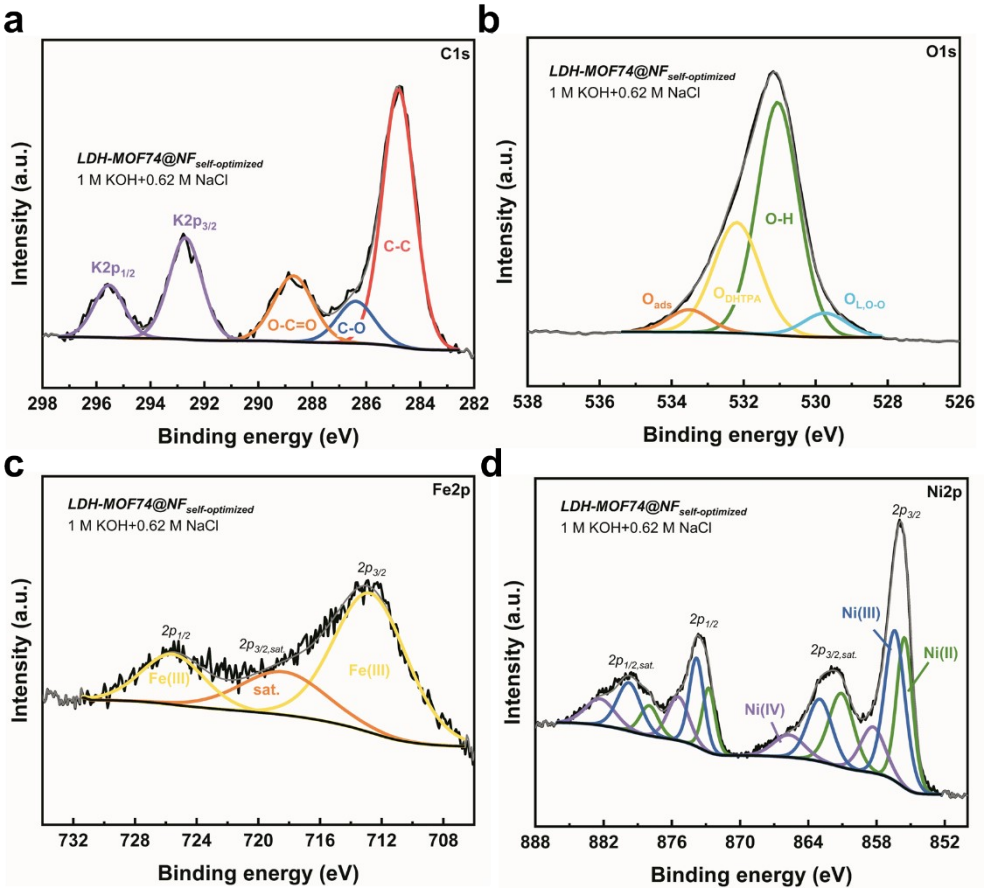

Figure S10. Fine XPS Spectra of (a) C1s, (b) O1s, (c) Fe2p, and (d) Ni2p of LDH-MOF74@NF after OER test in 1 M KOH + 0.62 M NaCl.

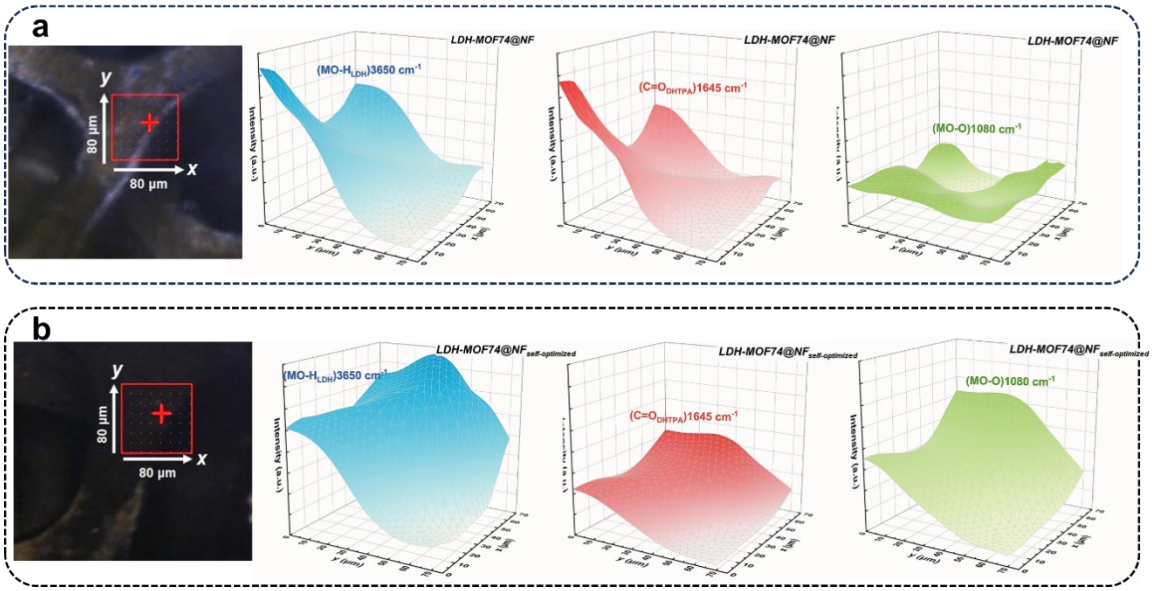

Figure S11. Mapping results of micro-IR spectroscopy at 3650 cm^{-1}, 1650 cm^{-1}, and 1080 cm^{-1} for (a) LDH-MOF74@NF and (b) after self-optimization.

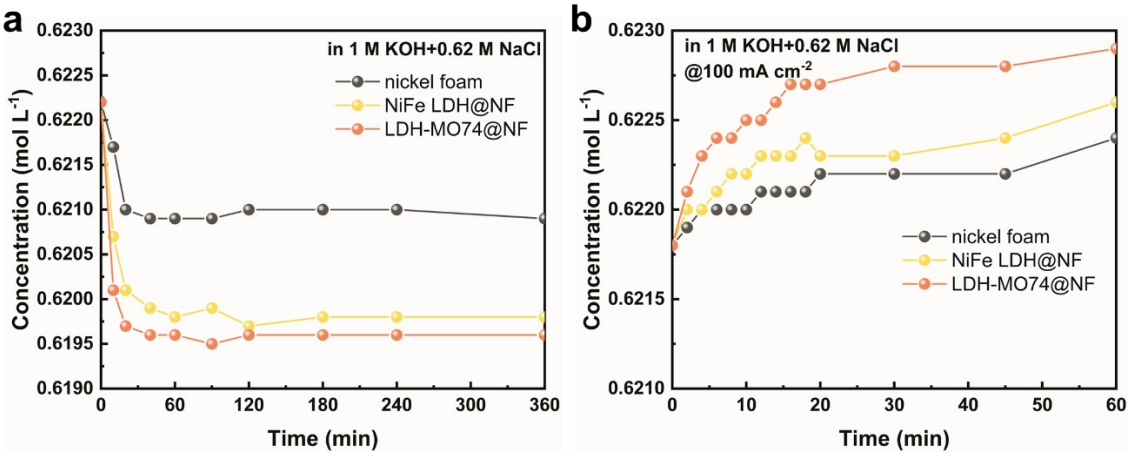

Figure S12. (a) The Cl^- adsorption of electrodes immersed in alkaline seawater. (b) Chloride concentration during electrolysis@100 mA cm^{-2} for electrodes wiht saturated Cl- adsorption.

Reference

1. G. Dong, F. Xie, F. Kou, T. Chen, F. Wang, Y. Zhou, K. Wu, S. Du, M. Fang and J. C. Ho, *Mater. Today Energy*, 2021, **22**, 100883.
2. J. Cai, X. He, Q. Dong, Y. Li, P. Su, D. Qu, J. Liu, Y. Lu, Q. Jin and Z. Sun, *Surf. Interfaces*, 2024, **51**, 104772.
3. Y. Yang, S. Wei, Y. Li, D. Guo, H. Liu and L. Liu, *Appl. Catal., B*, 2022, **314**, 121491.
4. Y. S. Park, J.-Y. Jeong, M. J. Jang, C.-Y. Kwon, G. H. Kim, J. Jeong, J.-h. Lee, J. Lee and S. M. Choi, *J. Energy Chem.*, 2022, **75**, 127-134.
5. S. Song, Y. Wang, P. Tian and J. Zang, *J. Colloid Interface Sci.*, 2025, **677**, 853-862.
6. P. Ding, H. Song, J. Chang and S. Lu, *Nano Research*, 2022, **15**, 7063-7070.
7. M. Xiao, C. Wu, J. Zhu, C. Zhang, Y. Li, J. Lyu, W. Zeng, H. Li, L. Chen and S. Mu, *Nano Research*, 2023, **16**, 8945-8952.
8. J. Qian, Y. Zhang, Z. Chen, Y. Du and B.-J. Ni, *Chemosphere*, 2023, **345**, 140472.
9. Z. Li, M. Liu, J. Yan and L. Y. S. Lee, *Chem. Eng. J.*, 2023, **473**, 145293.
10. F. Sun, Y. Wang, X. Tian, R. Zhu, Z. Hou, Y. Zheng, J. Zang and L. Dong, *J. Catal.*, 2024, **437**, 115655.